

caution in light of the data distribution shown in Appendix 6.C. The spatial pattern is consistent across seasons. Model predictive ability was good, with low white noise, excellent overall ROC performance, and excellent performance in the ‘high’ certainty class that dominated the study area. Model predictions were more uncertain and variable in fall, when the species was less abundant.

Cory’s Shearwater (*Calonectris diomedea*)

Cory’s Shearwater (Figure 6.11, Tables 6.18-20) is a large seabird found across the Northern Atlantic and seldom seen near land except during breeding. Since it breeds on islands in the eastern North Atlantic and Mediterranean, it is not regularly seen close to shore in North America. It is commonly found where water masses mix. Most sightings in the study area are made during the summer and fall. Abundance predictions peak offshore and the abundance trend follows a general southwest to northeast pattern along the shelf edge, with a more expansive distribution to the north and east. The apparent hotspots south of Block Island and near Nantucket Shoals are not well-supported by data (they are based primarily on extrapolation of environmental relationships) and therefore should be considered hypothetical until tested with additional survey data. Model predictive ability indicated by error statistics and ROC analysis is fair to good where certainty is high. However, the white noise component of the model is moderately high indicating a high degree of unpredictable random variability in abundance at any given location. This is consistent with findings of the more recent Rhode Island SAMP study, which found significant interannual variation in the abundance of this species in offshore areas (Paton et al., 2010). It should also be noted that this species is attracted to fishing vessels and may be influenced by fishing patterns.

Dovekie (*Alle alle*)

Dovekies (Figure 6.12, Tables 6.21-23) are almost strictly pelagic, coming ashore only to breed on cliffs in areas far north of the NY Bight. Sightings are uncommon in the study area except offshore in winter, but when Dovekies are seen, they exhibit clear spatial and temporal patterns. Dovekies are most common in the winter months and there is an obvious preference for warmer waters above the shelf slope and in the middle of the study area, northwest of Hudson Canyon. This is consistent with Dovekie’s tendency to concentrate in this region near temperature fronts and aggregations of copepods and similarly sized zooplankton (D. Veit, pers. comm.). Model predictive ability in ROC analysis was fair to good; abundance when sighted was highly variable (high Stage II white noise). This species may recently have increased in abundance (e.g., Paton et al., 2010) and the patterns depicted here should be compared to more recent data.

Great Black-Backed Gull (*Larus marinus*)

The Great Black-Backed Gull (Figure 6.13, Tables 6.24-26) is a coastal species found in the North Atlantic and Palearctic, breeding on coasts in North America and Europe. The study area is towards the southern limit of this species’ distribution (breeds south to North Carolina; ranges to Florida in winter), which may explain why sightings are more common in the northern part of the study area. Most sightings are made between July and November during breeding months and there are confirmed observations of breeding on Long Island. Relatively certain predictions of high abundance were made throughout the northeast portion of the study domain, including the vicinity of Block Island southeast to the shelf edge, and Martha’s Vineyard south to the shelf edge. High abundances were also predicted near the coast and along the shelf edge. The onshore-offshore distribution varied somewhat with season (Appendix 6.C). Though highly variable (white noise component was high), presence predictions were generally excellent and error statistics were acceptable even for the ‘low’ certainty class.

Great Shearwater (*Puffinus gravis*)

The Great Shearwater (Figure 6.14, Tables 6.27-29) is one of only a few species found in the NY Bight that migrate from breeding grounds in the Southern Hemisphere to wintering grounds in the Northern Hemisphere. Migration follows a quasi-circular route moving up the western edge of the Atlantic in spring-summer and returning along the eastern Atlantic. Sightings in the study area occur primarily in summer and fall. Low abundance was predicted over most of the study area, suggesting that the birds remain primarily offshore during migration and generally follow the shelf edge. A broad, moderate concentration of abundance occurs in the center of the NY planning area, just south of Long Island extending south and southeast to the shelf edge and east past Nantucket Shoals. This pattern of abundance is similar to that of other shearwaters (e.g., Cory’s

Shearwater). Presence predictions were fair to good; abundance when seen was highly variable (high white noise). Error statistics were fair to good in higher certainty classes.

Herring Gull (*Larus argentatus smithsonianus*)

The Herring Gull (Figure 6.15, Tables 6.30-32) is a very widespread and abundant seabird in the study area. It is a year-round resident and breeds along the coasts. Especially high abundance occurs at the mouth of the Hudson River, along the south shore of Long Island, south of Nantucket at the eastern edge of the domain, and scattered other locations throughout the domain. This species is attracted to ships, and the high abundances off New York Harbor and south of Martha's Vineyard may be due to birds aggregating at fishing trawlers (and thus not reliable long-term hotspots). A clear and dramatic change in spatial distribution occurs over the course of a year (see Appendix 6.C). Sightings are distributed across the shelf during winter, spring and fall, but are rare greater than 50 km from shore during the summer breeding months. Very high white noise components indicate a highly variable, transient pattern of distribution, and error statistics are correspondingly poor; however, the model predicted the range of variability well (%1SD statistics) and ROC statistics were excellent in the 'medium' certainty class.

Laughing Gull (*Leucophaeus atricilla*)

The Laughing Gull (Figure 6.16, Tables 6.33-35) breeds along the eastern Atlantic with the greatest abundances seen south of the study area, though it is fairly common in NY. The study area is relatively close to the northern limit of the Laughing Gull breeding distribution (which extends as far north as Nova Scotia and New Brunswick). Predictions of highest abundance and occurrence are made within 50 km of shore and near the Hudson River and New Jersey coasts, and are consistent across spring, summer, and fall seasons. Sightings in the winter and early-spring are more rare; this species winters in the mid-Atlantic and to the south. Model predictions of presence are excellent, though abundance when seen is fairly variable. Predictions in the 'high' certainty class are excellent; 'medium' certainty predictions are less good.

Northern Fulmar (*Fulmarus glacialis*)

The Northern Fulmar (Figure 6.17, Tables 6.36-38) is a gull-like relative of albatrosses and shearwaters. Most sightings are made between January and June (winter-spring). The majority of sightings are offshore, between 75 km from shore and the shelf edge, although sightings occur somewhat closer to shore in the northeast of the study area, offshore of Martha's Vineyard and Nantucket. Patterns are consistent across seasons. Performance in ROC analysis was good, and diagnostics are excellent for the high certainty class which covers about half the study area.

Northern Gannet (*Morus bassanus*)

The Northern Gannet (Figure 6.18, Tables 6.39-41) is one of the most abundant and widespread species of seabird in the study area. It is frequently sighted between October and April and exhibits distinct spatial patterns among seasons, with more offshore sightings in spring. In the winter most individuals are seen in the mid-to-inner shelf towards the southern part of the domain, in the spring throughout the domain and especially along the shelf edge, and in the fall in the inner to mid-shelf with peaks near Nantucket Shoals and Long Island. This species is known to aggregate to areas of fishing activity, and so its spatial distribution may have changed since the 1980's with shifting patterns of fishing effort. In particular, large aggregations of Northern Gannets were observed in association with foreign factory trawler boats in the 1980's, and similar aggregations have not been observed since those boats stopped frequenting the region (D. Veit, pers. comm.). Thus, the hotspots near the shelf break require confirmation from more recent data before being considered persistent aggregations. Both the two-pulse fall and spring migrant pattern and the tendency to aggregate to fishing boats have been confirmed by recent studies in the area (Paton et al., 2010). Model predictive performance is poor to fair, depending on certainty class; the Stage II white noise component (unpredictability in abundance when present) is very high.

Pomarine Jaeger (*Stercorarius pomarinus*)

The Pomarine Jaeger (Figure 6.19, Tables 6.42-44) is a skua occasionally seen offshore of New York in the fall (<4% frequency). Very few sightings are made in other seasons. Areas of highest abundance are predicted along the shelf edge, and south of Nantucket shoals. It is possible that these aggregations are due to the presence of fishing trawlers and are not reliable long-term hotspots (D. Veit, pers. comm.). This species is

seldom if ever observed close to shore. Model predictive performance was excellent for the high certainty class, but model uncertainty tended to underestimate uncertainty seen in cross-validation, due to the highly skewed abundance distribution.

Sooty Shearwater (*Puffinus griseus*)

The Sooty Shearwater (Figure 6.20, Tables 6.45-47) breeds on islands off southern South America and New Zealand and spends summers in the North Pacific and Atlantic. Most sightings in the study area are between April and July (spring-summer). Predictions show a clear preference for the shelf edge during the spring, similar to other shearwaters in the study area. Predictions of high abundance are also made in discrete areas in the spring and summer south of central Long Island and south of Nantucket Island, respectively. Model performance was generally fair, but excellent in the ~20% of the study area with 'high' certainty.

Wilson's Storm-Petrel (*Oceanites oceanicus*)

Wilson's Storm-Petrel (Figure 6.21, Tables 6.48-50) is one of the most common species seen in summer in the study area, and is also present in spring and fall. It breeds in Antarctic and sub-Antarctic seas, but ranges to the Northern Pacific, Atlantic and Indian Oceans during summer months. The majority of sightings in the study area are between May and September (spring, summer, and fall). Areas of high abundance are predicted fairly uniformly over the shelf, increasing offshore. Abundances extend into the nearshore in the northern part of the study area in summer. Though white noise is high, indicating a high degree of unpredictability in abundance, ROC analysis showed good predictive ability. Model diagnostics in the 'high' certainty class indicated excellent performance.

6.9.2. Group notes

Less Common Alcids

The Less Common Alcids group (Figure 6.22, Tables 6.51-53) includes the Atlantic Puffin, Common Murre, Razorbill, Thick-billed Murre, and unidentified species in the Family Alcidae. These species are generally rare in the study area, though frequency of sightings reaches 5% in winter. They occur in winter and spring, and very rarely in fall. Predictions are uncertain and cross-validation results are poor. Generally there appears to be an area of elevated abundance along the shelf especially in the northeast of the domain, south of Nantucket shoals. ROC analysis shows very little predictive success, though more certain predictions do have better cross-validation error statistics, indicating that when the group is present the abundance predictions are fairly good. The Rhode Island SAMP study found that the Razorbill and Common Murre have become much more common than earlier surveys in this region in recent years, so analysis of newer survey data will be important to an improved assessment of this group (Paton et al., 2010).

Coastal Waterfowl

Coastal Waterfowl (Figure 6.23, Tables 6.54-56), as defined here, are a diverse group including scoters, ducks, mergansers, eiders and other waterfowl in the family Anatidae, plus Red-throated Loons (family Gaviidae). We note that loons are not generally considered to be waterfowl (usually this term refers to species in the family Anatidae) but are included here because the Red-throated Loon sightings in the Manomet dataset were spatio-temporally similar to the true waterfowl sightings in the region, and Red-throated Loons were not seen enough to model separately (likely due in part to their low detectability; these birds tend to dive when moving ships are approaching [P. Paton, pers. comm.]). These species occur near coastlines and islands throughout the study area, both inside and outside of Long Island Sound, northeast around Block Island, Nantucket, and Martha's Vineyard, and southwest along the NJ shore. Highest abundances are seen in spring. Distributions are generally consistent across seasons. Statistically, model performance is generally excellent, especially with regard to occurrence. Error statistics are good in the high certainty class, except the model-predicted confidence intervals under-predict error (the %1SD statistic is well below its theoretical target of 68.3%). However, there are significant caveats. Stage II white noise is high, indicating that although occurrence is highly predictable, the observed abundance when seen exhibits a high degree of unpredictable random variability. Moreover, because the Manomet dataset had very few nearshore surveys in winter when seaducks are most abundant, and also because Red-throated Loons and seaducks tend to avoid ships, the winter estimate of abundance for this group is likely to be a severe underestimate. Finally, because this group encompasses a large number of species, species-specific inferences cannot be made. If particular species of waterfowl are

of concern, additional data will be necessary to facilitate species-specific modeling. We note that much better data sources exist for wintering seabirds (e.g., Zipkin et al., 2010).

Jaegers

Jaegers (Figure 6.24, Tables 6.57-59) are rare in the study area, only exceeding a frequency of 0.5% in fall (when they reach a frequency of 2%). They are occasional in spring and summer and absent in winter. The only season for which sufficient data were available to model was fall. The model performs fairly well for high certainty areas, given limited data, but the high abundances predicted at the edges of the domain (along the shelf edge) have low certainty. ROC analysis indicates high sensitivity but with a high false positive rate. Other cross-validation statistics suggest caution is necessary in applying this model.

Phalaropes

Phalaropes (Figure 6.25, Tables 6.60-62) were only present at high enough frequency to model in spring. They are pelagic in distribution, concentrating at the shelf edge, especially in the central and eastern part of the domain. Model performance is good to excellent especially in the high certainty class that covers half the domain. Model-predicted uncertainty bounds tend to underestimate observed variability in abundance when seen.

Less Common Shearwaters

The Less Common Shearwaters (Figure 6.26, Tables 6.63-65) group includes the Manx Shearwater, Audubon's Shearwater and unidentified species in the Family Procellariidae. Most sightings occur in the spring, summer and fall, with a peak in summer. Highest abundance is predicted in summer along the eastern end of Long Island and Block Island and near Nantucket Shoals, though uncertainty is high for some of these areas. Otherwise, scattered sightings are made offshore out to the shelf edge throughout the study area in spring, summer, and fall. Audubon's Shearwaters are more common offshore, where they are mixed with Manx Shearwater sightings. Manx Shearwaters dominate nearshore sightings off the eastern tip of Long Island. Abundance and frequency are generally greater in the center and northeast than the southwest of the region. However, model performance in cross-validation is poor and results of this model should be used with caution.

Less Common Small Gulls

The Less Common Small Gulls (Figure 6.27, Tables 6.66-68) group includes the Ring-billed Gull and Bonaparte's Gull. The group is fairly rare in the study area (<4%); most prevalent in the fall and winter. Both of these species are migrants passing through the area in these seasons; summer breeding grounds are in boreal North America. High abundances are predicted along the Hudson shelf valley and to its south, and near the east end of Long Island. Insufficient sightings were made in very nearshore coastal areas to characterize distribution accurately, as indicated by the high uncertainty in these areas. Spatial distribution was consistent across seasons. Model performance in cross-validation was fair.

Less Common Storm-Petrels

The Less Common Storm-Petrels group (Figure 6.28, Tables 6.69-71) includes the Leach's Storm-Petrel, Band-rumped Storm-Petrel, White-faced Storm-Petrel (rarely), and unidentified species in the Family Hydrobatidae. Species in this group are very rare except in summer, when frequency of sighting approaches 5%. Areas of highest predicted abundance are scattered offshore along the shelf edge, slightly higher toward the south. Distribution is fairly consistent across seasons, with a subtle southward shift in summer. Occasional sightings occur at the east end of Long Island, primarily in summer, and in the Hudson Shelf Valley vicinity. Leach's Storm-Petrel was the most common species sighted and the only one positively identified in the nearshore. Overall, model performance is fair to poor for SPUE, but presence prediction diagnostics are good for the 'high' certainty class. A very high Stage II white noise component means abundance when seen is very hard to predict.

Less Common Terns

The Less Common Terns group (Figure 6.29, Tables 6.72-74) includes the Roseate, Least, Royal, Arctic, Sooty, Bridled, Caspian, and Forster's Terns and unidentified species in the Family Sternidae. The first two species are listed as endangered and threatened, respectively, by New York. The Roseate Tern is also federally listed

as Endangered by the USFWS. Most sightings are in the summer breeding months and are within 50 km of shore. Cross-validation shows presence/absence predictions are acceptable, but abundance predictions are poor except for the most certain areas (generally places far offshore where the species' are virtually certain to be absent). Given the sample sizes used to fit these models and the marginal performance statistics, caution should be used in applying SPUE predictions; presence/absence predictions can be used, but should also be treated with some caution. Caution should also be exercised because this group lumps many species, some of which are known to have different spatial distributions, and because the group contains more "Unidentified Tern" sightings than positively identified species sightings. These model results should be used as a starting point for forming hypotheses about distribution patterns which should be tested with further sampling and combined with additional species-specific survey data and expert opinion before being used for decision-making purposes. We note that Caspian Terns are now commonly seen in Rhode Island waters (Paton et al., 2010), but no Caspian Terns were positively identified in the Manomet dataset.

Unidentified Gulls

The Unidentified Gulls group (Figure 6.30, Tables 6.75-77) could consist of a variable set of species depending on the location within the study area and the time of year. This group had enough sightings to model in fall, winter, and spring, but not summer, suggesting that its members breed elsewhere and are passing through the area in spring/fall or overwintering. Another possibility is that many of the unidentified gulls could be juveniles; juvenile gulls can be very difficult to identify. The low numbers in summer are consistent with this hypothesis as young gulls would not yet be fledged at that point. The peak predicted abundance is in fall near Martha's Vineyard. Abundance is also predicted nearshore throughout the study area (with smaller peaks near the mouth of Long Island Sound, near Nantucket Shoals, and near New York Bay). This pattern is fairly consistent across seasons. Cross-validation performance is acceptable to good in the medium and high uncertainty classes, though there is high white noise in Stage I and the model-predicted confidence intervals are too small (low %1SD). Overall, model results for this group should be treated with caution as the identity of the component species is unknown, possibly variable over time and space, and possibly overlapping with some of the other, positively identified, gull species and groups that were modeled separately.

6.9.3. Non-modeled species groups

Cormorants

Cormorants (Figure 6.31, Table 6.78) are infrequent in the Manomet database, due in part to poor sampling in very nearshore areas. Point sightings of cormorants are most common in winter and are clustered near the east end of Long Island, Block Island, Martha's Vineyard, New York Bay, and southwest of Great Peconic Bay. More data is necessary to assess the spatial distribution of cormorants in offshore waters of NY if they are of particular interest. In the winter, when most common, unidentified birds were probably mainly Great Cormorants (P. Paton, pers. comm.).

Rare Visitors

The Rare Visitors group (Figure 6.32, Table 6.79) consists of species that are non-breeding, transient, and rare in the study area. Sightings are very infrequent (<1% total) and scattered around the study area with little obvious spatial pattern. If any of these species (listed in Table 6.2) are of particular interest, detailed additional studies will have to be performed.

Less Common Skuas

The Less Common Skuas group (Figure 6.33, Table 6.80) includes the Great Skua and unidentified sightings of skuas (species in the family Stercorariidae that are not Jaegers). The unidentified skuas are very likely to have been either poorly seen Great Skuas or South Polar Skuas, as these are the only two skua species recorded in the western North Atlantic. Sightings of this group are very infrequent in the study area (<1%). Most sightings are in the fall months, similar to the Pomarine Jaeger. Sightings generally occur offshore along the outer continental shelf, and are slightly more concentrated toward the south-central part of the domain near the shelf. If the Great Skua or other skuas thought to be represented by this group are of particular concern, more detailed studies or additional data collection and modeling should be conducted.

6.9.4. 'No birds sighted'

Figure 6.34A shows the annual predicted index of abundance of surveys that result in no sightings of seabirds (measured by multiplying the predicted probability of occurrence by the predicted transect area in which no birds were detected, in km²). Figure 6.34B shows the probability of at least one survey in any season resulting in "no birds sighted" (i.e., the annual integrated presence probability, calculated as if the 'no birds sighted' category were a species). Tables 6.81, 6.82, and 6.83 summarize the input data, predictors, and diagnostic statistics, respectively, for the 'no birds sighted' model.

The eastern end of Long Island and areas near Block Island and Martha's Vineyard have a lower probability than average of experiencing times without seabirds (i.e., most surveys in these areas see seabirds). The inner shelf in the Long Island Platform vicinity, about 10-30 km offshore, has an above average probability of experiencing times without seabirds. The patterns vary somewhat from season to season, and predictive performance of the model is fair to poor (high white noise, marginal error statistics). The reader should be particularly cautious of high predicted "no birds sighted" values within 10 km of shore as Manomet survey coverage drops off rapidly in the nearshore. Nonetheless, there are discernible spatial patterns that may be useful as an alternative to abundance hotspot maps to identify areas of potentially reduced conflict between ocean uses and seabirds.

6.9.5. Hotspots

Predicted hotspots of abundance for all modeled species combined (Figure 6.35) occur along the coast, especially along the Hudson Shelf Valley and in scattered areas throughout the shelf, particularly near Nantucket Shoals. The onshore-offshore gradient in abundance is consistent with many previous studies of seabirds in this region, and recent intensive survey work in New Jersey and Rhode Island.

Species richness hotspots (Figure 6.36) are scattered throughout the center and northeast of the study area, extending south-southeast from Long Island to the shelf edge, and between Long Island and Nantucket Shoals. Low diversity predicted beyond the shelf edge is unreliable, as indicated by the uncertainty overlay. Very nearshore predictions are also unreliable throughout the domain. This is consistent with increased species richness along the Atlantic Flyway. The patchy, uneven pattern of the species richness predictions is a result of the discrete nature of this variable (there can only be whole numbers of species) combined with the necessity of choosing a somewhat arbitrary threshold to define a species as present or absent at a given location.

The predicted Shannon diversity index (Figure 6.37) shows a smoother pattern that is distinct from the richness and abundance patterns. It reveals hotspots and coldspots of diversity scattered throughout the shelf, with highest diversity in the northeast of the study area near Nantucket and at the mouth of Long Island Sound.

It is important to remember that concentrations of abundance and diversity can form and disperse rapidly, because seabirds are highly mobile, and interact with dynamic ecological resources and processes. Thus, the patterns displayed here reflect the considerable variability in concentrations of seabird abundance over the 9-year observation period (1980-1988). For example, hotspots may form in entirely different locations in different years resulting in multiple hotspots in the final map, not all of which form in any given year or season. It is also important to note that uncertainty accumulates when predictive statistical models are combined, a fact that is reflected in the uncertainty maps. Reliable hotspot predictions can only be produced in places where data is sufficiently dense for all species.

6.9.6. Point Maps of Seabirds of Concern

Figure 6.38 shows the locations of sightings for four species of particular concern: the Roseate Tern, Common Tern, Least Tern, and Common Loon. The Piping Plover, listed as endangered by New York, was not in the Manomet dataset and therefore was not mapped. Most species of concern are sighted within 50 km of shore. Noticeable concentrations of sightings occur south of Jamaica and Great South bays. It is important to note that Figure 6.38 presents point sightings, not results of a predictive model. No information can be assumed regarding the presence or absence of the species in between sample points. With the exception of the Common Loon, these species were too rare to produce individual species predictive models. The remaining species were included in the predictive model for "Less Common Terns."

Black-legged Kittiwake (*Rissa tridactyla*)

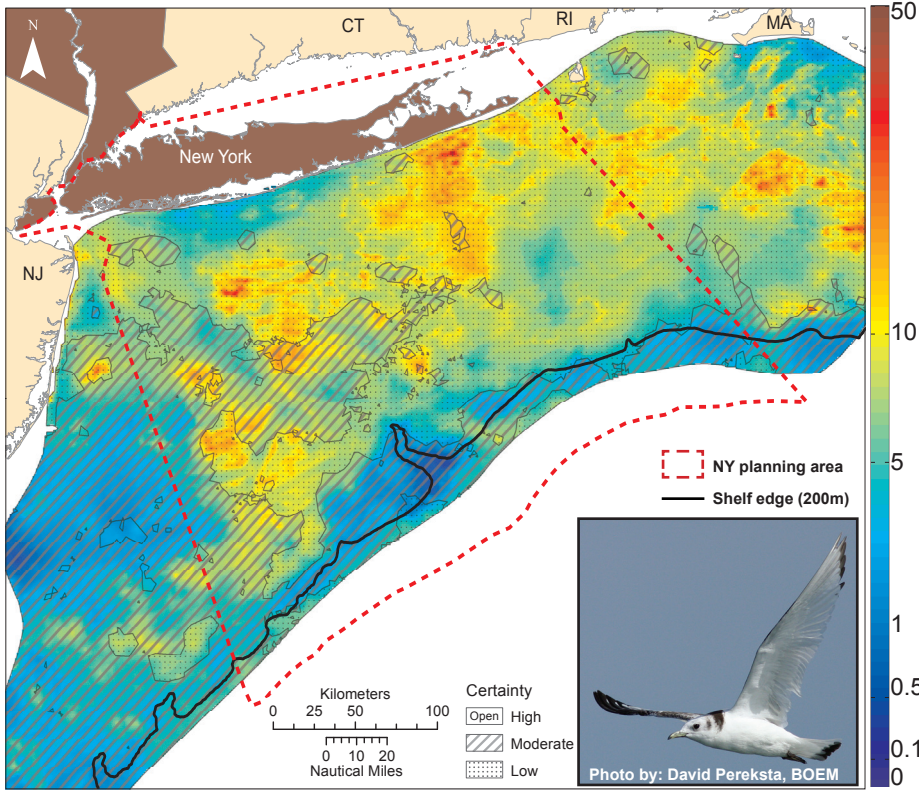


Figure 6.8. Predicted annual average relative index of abundance (SPUE, # indiv./ km²/15-min) for Black-legged Kittiwake, with certainty classes overlaid.

Table 6.9. Data table: Black-legged Kittiwake.

Statistic	SP	SU	FA	WI	All
N obs.	195	2	347	546	1090
Freq. (%)	7.7%	0.1%	12.5%	47.6%	11.9%
SPUE when present (No. indiv./ km ² /15 min.)					
Mean	9.17	0.96	6.29	8.17	7.73
10th%ile	1.47	0.20	1.09	1.76	1.45
Median	4.40	0.96	4.24	4.80	4.60
90th%ile	19.96	1.73	13.62	16.20	16.27
Max	121.59	1.73	57.90	153.44	153.44

Table 6.10. Predictor table: Black-legged Kittiwake.

Predictor	Occurrence				Abundance			
	Sp	Su	Fa	Wi	Sp	Su	Fa	Wi
BATH								
SLOPE								
DIST								
SSDIST								
SST								
STRT								
TUR								
CHL								
ZOO								
SLPSLP								
PHIM								

Table 6.11. Diagnostic table: Black-legged Kittiwake.

Diagnostic statistic	Certainty class			ALL
	Low	Med.	High	
%area	84%	16%	0%	Avg. LOW
Rank R	0.16	-0.13	n/a	0.02
%1SD	81.2%	90.0%	n/a	84.0%
AUC	0.63	0.64	n/a	0.47
p(AUC)	0.02	0.06	n/a	0.70
MAPE	141%	134%	n/a	145%
Rel.MAE	44%	42%	n/a	44%
Rel.RMSE	80%	67%	n/a	78%
Rel.Bias	25%	10%	n/a	14%
Bias Dir.	+	-	n/a	+

Common Loon (*Gavia immer*)

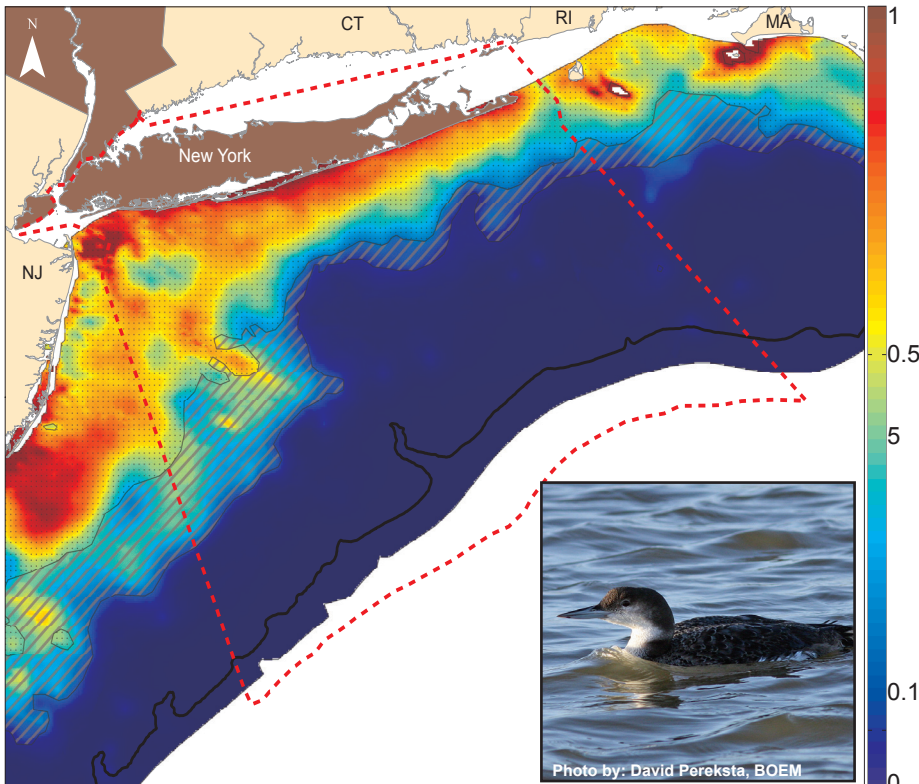


Figure 6.9. Predicted annual average relative index of abundance (SPUE, # indiv./ km²/15-min) for Common Loon, with certainty classes overlaid (see legend in Figure 6.8).

Table 6.12. Data table: Common Loon.

Statistic	SP	SU	FA	WI	All
N obs.	112	4	60	40	216
Freq. (%)	4.4%	0.1%	2.2%	3.5%	2.4%
SPUE when present (No. indiv./ km ² /15 min.)					
Mean	0.59	0.51	0.28	0.46	0.48
10th%ile	0.16	0.27	0.10	0.12	0.13
Median	0.36	0.49	0.18	0.24	0.27
90th%ile	0.92	0.80	0.54	1.17	0.80
Max	9.49	0.80	1.92	2.53	9.49

Table 6.13. Predictor table: Common Loon.

Predictor	Occurrence				Abundance			
	Sp	Su	Fa	Wi	Sp	Su	Fa	Wi
BATH								
SLOPE								
DIST								
SSDIST								
SST								
STRT								
TUR								
CHL								
ZOO								
SLPSLP								
PHIM								

Table 6.14. Diagnostic table: Common Loon.

Diagnostic statistic	Certainty class			ALL
	Low	Med.	High	
%area	30%	16%	54%	Avg. MED.
Rank R	0.08	0.33	n/a	-0.04
%1SD	16.0%	66.7%	n/a	33.3%
AUC	0.58	0.57	n/a	0.77
p(AUC)	0.13	0.27	n/a	0.00
MAPE	204%	90%	n/a	258%
Rel.MAE	40%	17%	n/a	40%
Rel.RMSE	82%	24%	n/a	67%
Rel.Bias	87%	27%	n/a	41%
Bias Dir.	+	+	n/a	+

Common Tern (*Sterna hirundo*)

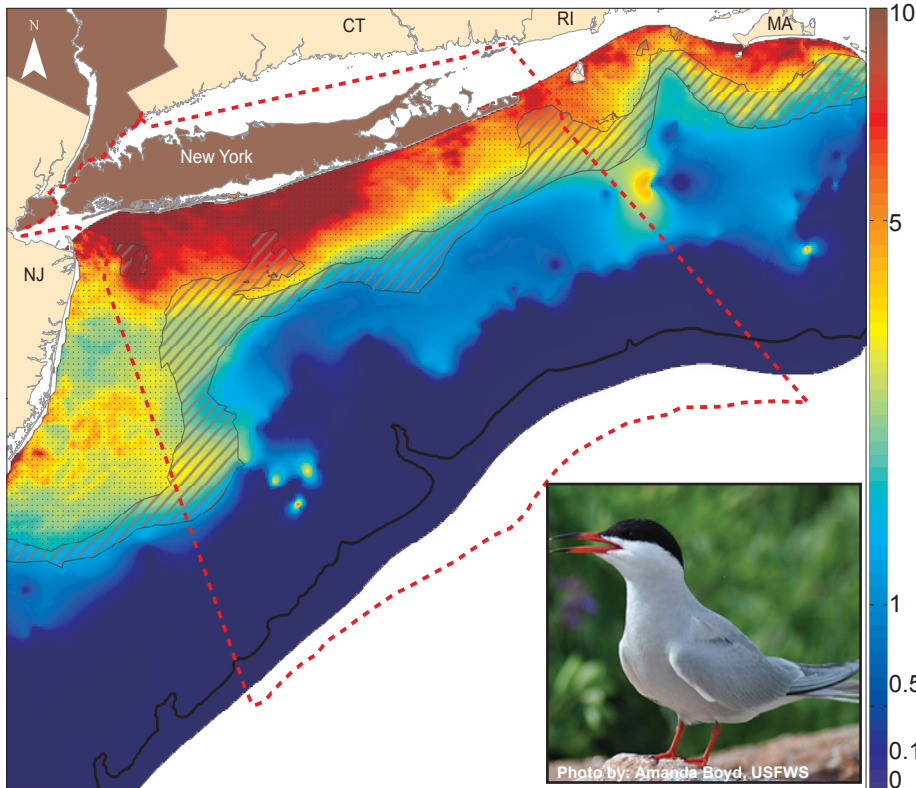


Figure 6.10. Predicted annual average relative index of abundance (SPUE, # indiv./km²/15-min) for Common Tern, with certainty classes overlaid (see legend in Figure 6.8).

Table 6.15. Data table: Common Tern.

Statistic	SP	SU	FA	WI
N obs.	56	76	32	1
Freq. (%)	2.2%	2.8%	1.2%	0.1%
SPUE when present (No. indiv./km ² /15 min.)				
Mean	6.61	5.08	3.88	0.27
10th%ile	0.48	0.28	0.33	0.27
Median	2.63	2.52	1.32	0.27
90th%ile	13.70	12.30	9.16	0.27
Max	48.43	27.20	20.16	0.27

Table 6.16. Predictor table: Common Tern.

Predictor	Occurrence				Abundance			
	Sp	Su	Fa	Wi	Sp	Su	Fa	Wi
BATH								
SLOPE								
DIST								
SSDIST								
SST								
STRT								
TUR								
CHL								
ZOO								
SLPSLP								
PHIM								

Table 6.17. Diagnostic table: Common Tern.

Diagnostic statistic	Certainty class			
	Low	Med.	High	ALL
	%area	%area	%area	Avg.
Rank R	24%	11%	65%	HIGH
%1SD	0.38	n/a	0.57	0.26
AUC	42.1%	n/a	71.4%	46.7%
p(AUC)	0.46	n/a	0.69	0.77
MAPE	0.68	n/a	0.05	0.00
Rel.MAE	298%	n/a	183%	579%
Rel.RMSE	37%	n/a	6%	24%
Rel.Bias	48%	n/a	10%	34%
Bias Dir.	54%	n/a	3%	18%
	+		+	+

Cory's Shearwater (*Calonectris diomedea*)

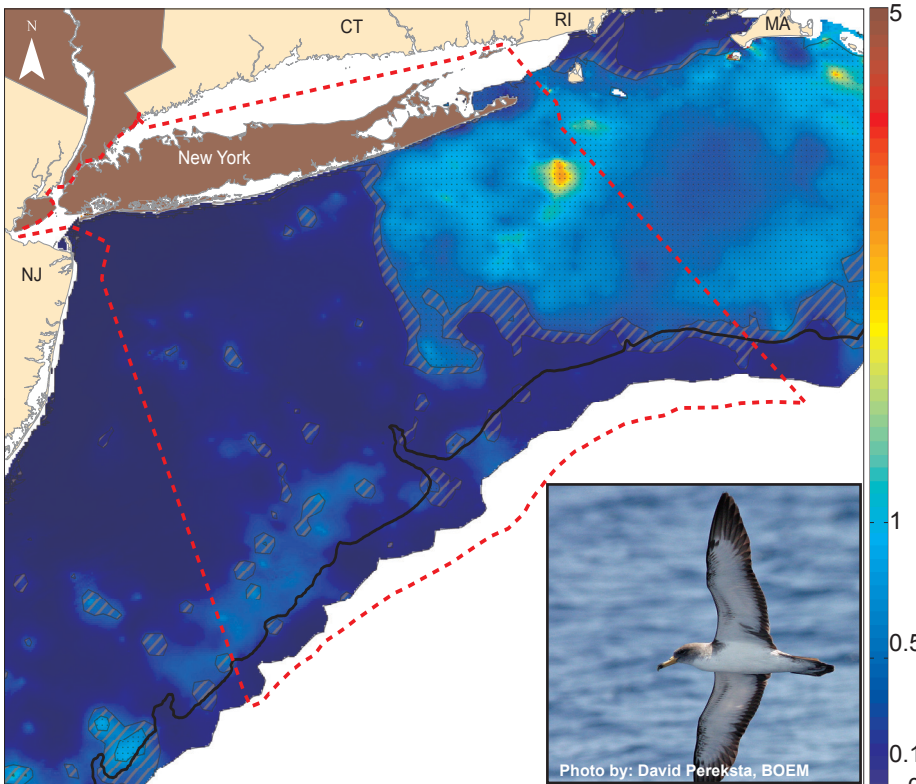


Figure 6.11. Predicted annual average relative index of abundance (SPUE, # indiv./km²/15-min) for Cory's Shearwater, with certainty classes overlaid (see legend in Figure 6.8).

Table 6.18. Data table: Cory's Shearwater.

Statistic	SP	SU	FA	WI	All
N obs.	3	297	153	1	454
Freq. (%)	0.1%	11.1%	5.5%	0.1%	5.0%
SPUE when present (No. indiv./km ² /15 min.)					
Mean	0.33	1.80	0.79	0.22	1.45
10th%ile	0.24	0.24	0.15	0.22	0.20
Median	0.30	0.65	0.45	0.22	0.60
90th%ile	0.45	2.40	1.44	0.22	2.16
Max	0.45	104.99	12.60	0.22	104.99

Table 6.19. Predictor table: Cory's Shearwater.

Predictor	Occurrence				Abundance			
	Sp	Su	Fa	Wi	Sp	Su	Fa	Wi
BATH								
SLOPE								
DIST								
SSDIST								
SST								
STRT								
TUR								
CHL								
ZOO								
SLPSLP								
PHIM								

Table 6.20. Diagnostic table: Cory's Shearwater.

Diagnostic statistic	Certainty class			
	Low	Med.	High	ALL
	%area	%area	%area	Avg.
Rank R	34%	16%	50%	MED.
%1SD	-0.03	-0.71	0.32	0.20
AUC	63.5%	80.0%	97.6%	78.6%
p(AUC)	0.57	0.55	0.67	0.64
MAPE	0.08	0.31	0.00	0.00
Rel.MAE	129%	115%	71%	112%
Rel.RMSE	35%	18%	11%	22%
Rel.Bias	101%	48%	31%	69%
Bias Dir.	8%	10%	1%	5%
	+	+	+	+

Dovekie (*Alle alle*)

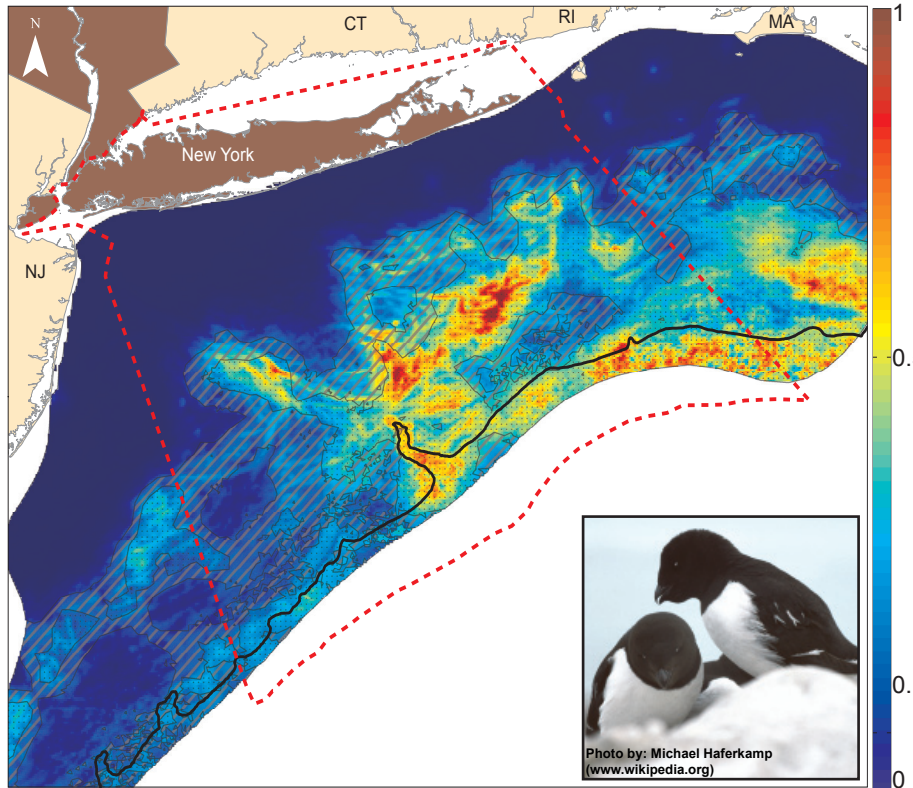


Figure 6.12. Predicted annual average relative index of abundance (SPUE, # indiv./km²/15-min) for Dovekie, with certainty classes overlaid (see legend in Figure 6.8).

*Note: Spring and Fall observations combined with Winter for modeling.

Table 6.21. Data table: Dovekie.

Statistic	SP*	SU	FA*	WI	All
N obs.	37	0	27	97	161
Freq. (%)	1.5%	0.0%	1.0%	8.4%	1.8%
SPUE when present (No. indiv./ km ² /15 min.)					
Mean	1.80	.	1.12	1.48	1.49
10th%ile	0.18	.	0.18	0.16	0.16
Median	0.90	.	0.60	0.56	0.65
90th%ile	5.17	.	3.01	3.10	3.13
Max	13.44	.	5.10	20.52	20.52

Table 6.22. Predictor table: Dovekie.

Predictor	Occurrence				Abundance			
	Sp	Su	Fa	Wi	Sp	Su	Fa	Wi
BATH								
SLOPE								
DIST								
SSDIST								
SST								
STRT								
TUR								
CHL								
ZOO								
SLPSLP								
PHIM								

Table 6.23. Diagnostic table: Dovekie.

Diagnostic statistic	Certainty class			
	Low	Med.	High	ALL
%area	33%	25%	42%	AVG. MED.
Rank R	-0.17	0.20	0.24	0.20
%1SD	58.6%	66.7%	63.6%	62.3%
AUC	0.51	0.68	0.71	0.71
p(AUC)	0.40	0.00	0.01	0.00
MAPE	231%	163%	237%	216%
Rel.MAE	9%	3%	3%	5%
Rel.RMSE	30%	6%	8%	15%
Rel.Bias	9%	7%	2%	5%
Bias Dir.	+	+	+	+

Great Black-backed Gull (*Larus marinus*)

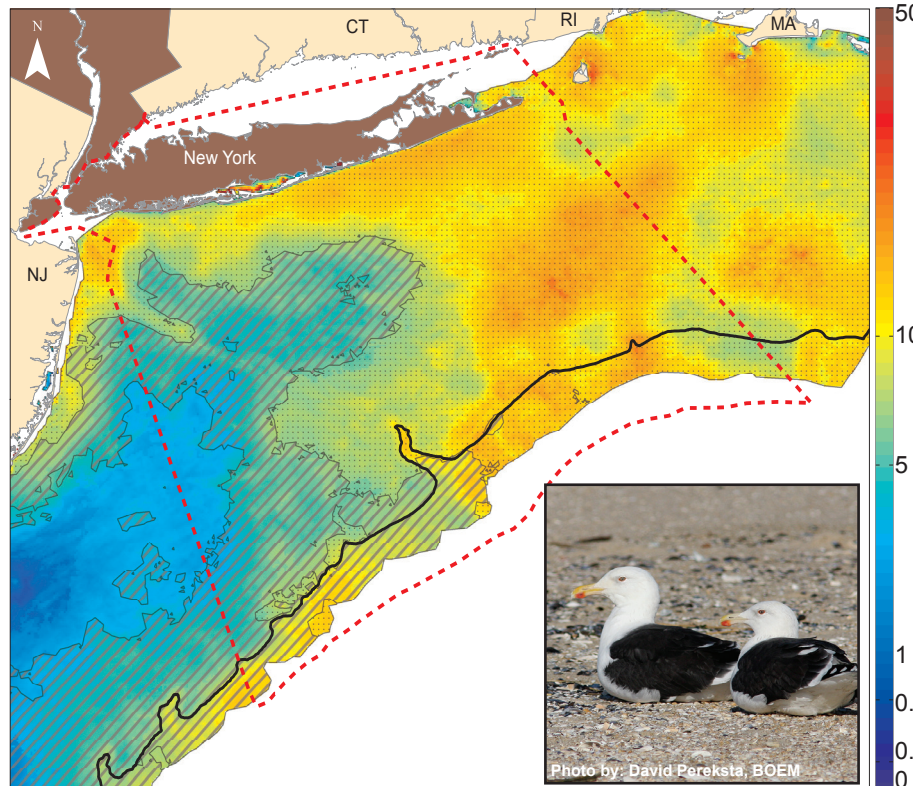


Figure 6.13. Predicted annual average relative index of abundance (SPUE, # indiv./km²/15-min) for Great Black-backed Gull, with certainty classes overlaid (see legend in Figure 6.8).

Table 6.24. Data table: Great Black-backed Gull.

Statistic	SP	SU	FA	WI	All
N obs.	624	149	506	468	1747
Freq. (%)	24.5%	5.6%	18.2%	40.8%	19.1%
SPUE when present (No. indiv./ km ² /15 min.)					
Mean	8.94	6.83	7.98	9.47	8.62
10th%ile	1.01	1.46	0.44	2.29	0.96
Median	5.10	5.40	4.80	5.87	5.22
90th%ile	16.23	12.80	17.10	19.50	17.10
Max	284.38	85.79	92.69	320.85	320.85

Table 6.25. Predictor table: Great Black-backed Gull.

Predictor	Occurrence				Abundance			
	Sp	Su	Fa	Wi	Sp	Su	Fa	Wi
BATH								
SLOPE								
DIST								
SSDIST								
SST								
STRT								
TUR								
CHL								
ZOO								
SLPSLP								
PHIM								

Table 6.26. Diagnostic table: Great Black-backed Gull.

Diagnostic statistic	Certainty class			
	Low	Med.	High	ALL
%area	60%	34%	6%	LOW
Rank R	0.23	0.37	-0.19	0.32
%1SD	87.7%	96.4%	100.0%	91.4%
AUC	0.40	0.55	1.00	0.77
p(AUC)	0.62	0.30	0.00	0.00
MAPE	148%	83%	294%	134%
Rel.MAE	42%	23%	17%	33%
Rel.RMSE	55%	36%	21%	46%
Rel.Bias	6%	11%	8%	7%
Bias Dir.	+	+	-	+

Great Shearwater (*Puffinus gravis*)

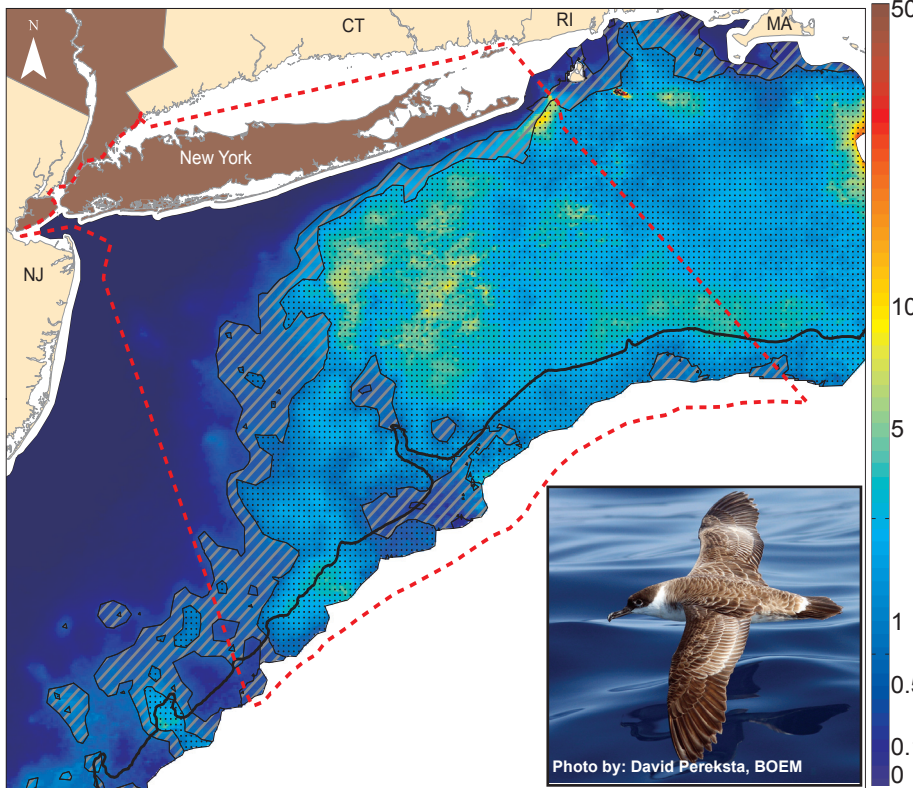


Figure 6.14. Predicted annual average relative index of abundance (SPUE, # indiv./km²/15-min) for Great Shearwater, with certainty classes overlaid (see legend in Figure 6.8).

Table 6.27. Data table: Great Shearwater.

Statistic	SP	SU	FA	WI	All
N obs.	33	497	404	9	943
Freq. (%)	1.3%	18.6%	14.5%	0.8%	10.3%
SPUE when present (No. indiv./ km ² /15 min.)					
Mean	0.98	2.80	1.75	0.29	2.27
10th%ile	0.14	0.27	0.22	0.18	0.24
Median	0.48	0.80	0.65	0.24	0.72
90th%ile	2.19	4.66	3.60	0.59	3.97
Max	2.88	223.54	79.19	0.80	223.54

Table 6.28. Predictor table: Great Shearwater.

Predictor	Occurrence				Abundance			
	Sp	Su	Fa	Wi	Sp	Su	Fa	Wi
BATH								
SLOPE								
DIST								
SSDIST								
SST								
STRT								
TUR								
CHL								
ZOO								
SLPSLP								
PHIM								

Table 6.29. Diagnostic table: Great Shearwater.

Diagnostic statistic	Certainty class			
	Low	Med.	High	ALL
	%area	%area	%area	Avg.
Rank R	0.04	0.03	0.21	0.07
%1SD	71.2%	92.6%	81.3%	75.6%
AUC	0.64	0.55	0.76	0.65
p(AUC)	0.00	0.22	0.00	0.00
MAPE	267%	89%	104%	221%
Rel.MAE	39%	16%	9%	27%
Rel.RMSE	85%	27%	27%	65%
Rel.Bias	1%	3%	2%	1%
Bias Dir.	-	+	-	-

Herring Gull (*Larus argentatus smithsonianus*)

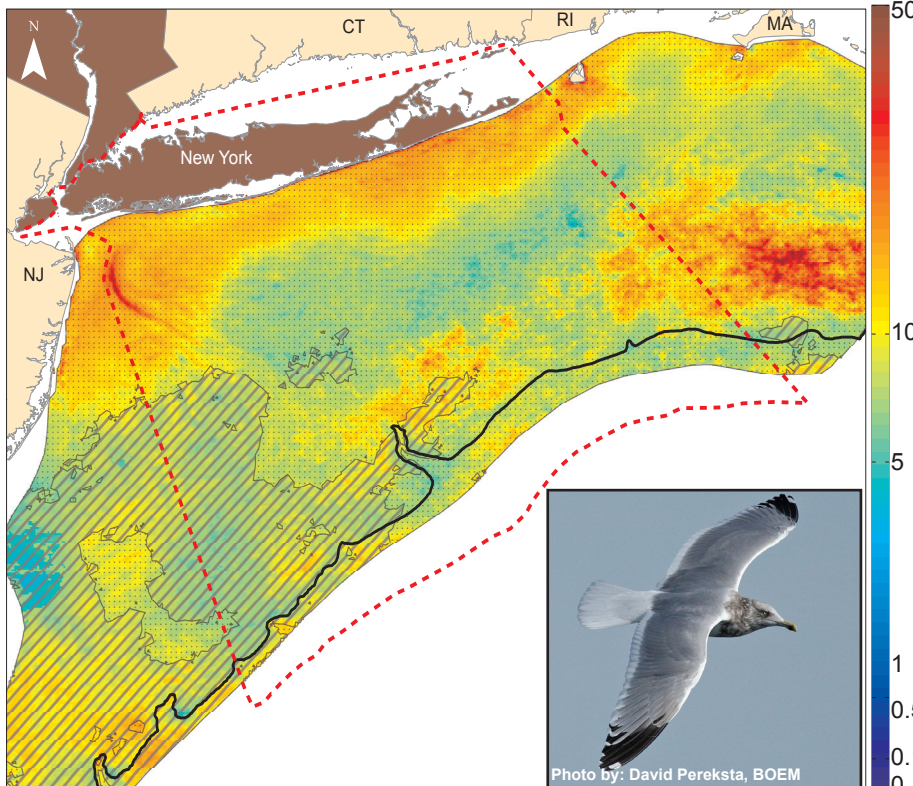


Figure 6.15. Predicted annual average relative index of abundance (SPUE, # indiv./km²/15-min) for Herring Gull, with certainty classes overlaid (see legend in Figure 6.8).

Table 6.30. Data table: Herring Gull.

Statistic	SP	SU	FA	WI	All
N obs.	1219	245	1128	580	3172
Freq. (%)	47.8%	9.2%	40.6%	50.5%	34.7%
SPUE when present (No. indiv./ km ² /15 min.)					
Mean	15.14	10.02	10.12	8.34	11.71
10th%ile	0.94	0.80	0.72	1.68	0.90
Median	7.20	5.20	6.35	5.76	6.30
90th%ile	27.85	19.35	21.60	15.93	22.29
Max	411.52	393.57	165.91	200.38	411.52

Table 6.31. Predictor table: Herring Gull.

Predictor	Occurrence				Abundance			
	Sp	Su	Fa	Wi	Sp	Su	Fa	Wi
BATH								
SLOPE								
DIST								
SSDIST								
SST								
STRT								
TUR								
CHL								
ZOO								
SLPSLP								
PHIM								

Table 6.32. Diagnostic table: Herring Gull.

Diagnostic statistic	Certainty class			
	Low	Med.	High	ALL
	%area	%area	%area	Avg.
Rank R	0.12	0.09	n/a	0.13
%1SD	81.7%	100.0%	n/a	82.8%
AUC	0.58	NaN	n/a	0.56
p(AUC)	0.24	NaN	n/a	0.32
MAPE	185%	61%	n/a	176%
Rel.MAE	45%	17%	n/a	43%
Rel.RMSE	74%	24%	n/a	70%
Rel.Bias	11%	8%	n/a	11%
Bias Dir.	-	-	-	-

Laughing Gull (*Leucophaeus atricilla*)

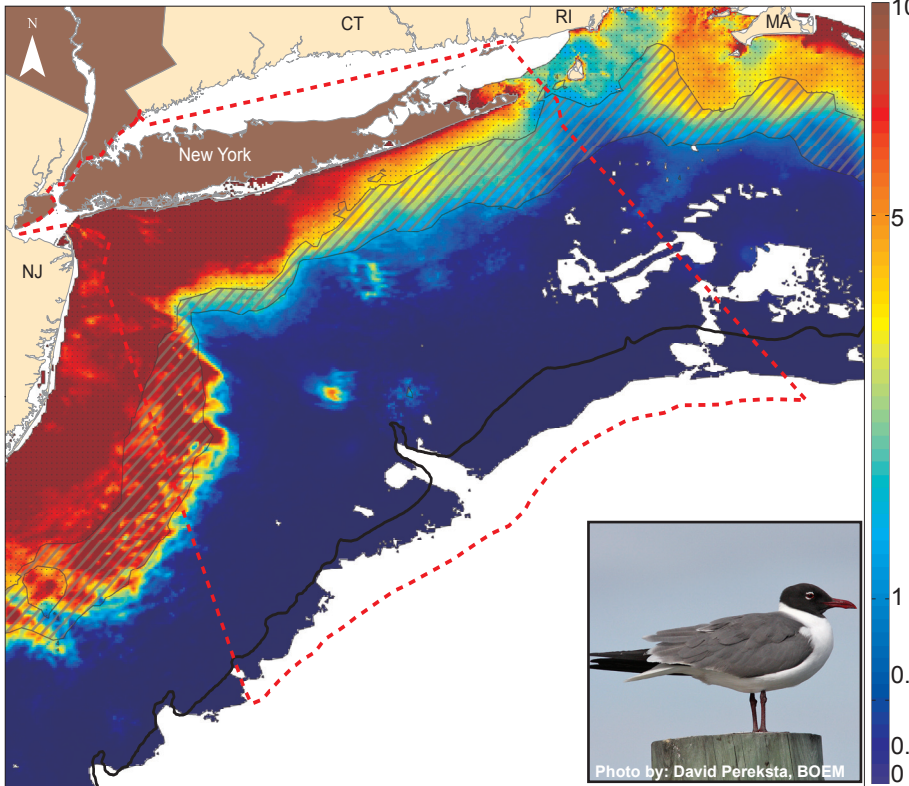


Figure 6.16. Predicted annual average relative index of abundance (SPUE, # indiv./ km²/15-min) for Laughing Gull, with certainty classes overlaid (see legend in Figure 6.8).

Table 6.33. Data table: Laughing Gull.

Statistic	SP	SU	FA	WI	All
N obs.	46	108	208	6	368
Freq. (%)	1.8%	4.0%	7.5%	0.5%	4.0%
SPUE when present (No. indiv./ km ² /15 min.)					
Mean	3.86	16.14	6.08	0.74	8.67
10th%ile	0.24	1.27	0.36	0.15	0.36
Median	2.76	10.08	3.52	0.70	4.52
90th%ile	8.35	36.96	13.74	1.54	19.73
Max	29.16	131.39	67.67	1.60	131.39

Table 6.34. Predictor table: Laughing Gull.

Predictor	Occurrence				Abundance			
	Sp	Su	Fa	Wi	Sp	Su	Fa	Wi
BATH	Green	Green	Red	White	Green	Green	Red	White
SLOPE	Green	Green	White	White	Green	Green	White	White
DIST	Green	Green	White	White	Green	Green	White	White
SSDIST	Green	Green	White	White	Green	Green	White	White
SST	Green	Green	Red	White	Green	Green	White	White
STRT	Green	Green	White	White	Green	Green	White	White
TUR	Green	Green	White	White	Green	Green	White	White
CHL	Green	Green	White	White	Green	Green	White	White
ZOO	Green	Green	White	White	Green	Green	White	White
SLPSLP	Green	Green	Red	White	Green	Green	White	White
PHIM	Red	Red	Red	White	Red	Red	White	White

Table 6.35. Diagnostic table: Laughing Gull.

Diagnostic statistic	Certainty class			
	Low %area 20%	Med. %area 18%	High %area 62%	ALL Avg. HIGH
Rank R	Green	Green	Green	Green
%1SD	Green	Green	Green	Green
AUC	Red	Green	Green	Green
p(AUC)	Red	Green	Green	Green
MAPE	Red	Green	Green	Green
Rel.MAE	Red	Green	Green	Green
Rel.RMSE	Red	Green	Green	Green
Rel.Bias	Red	Green	Green	Green
Bias Dir.	-	+	+	+

Northern Fulmar (*Fulmarus glacialis*)

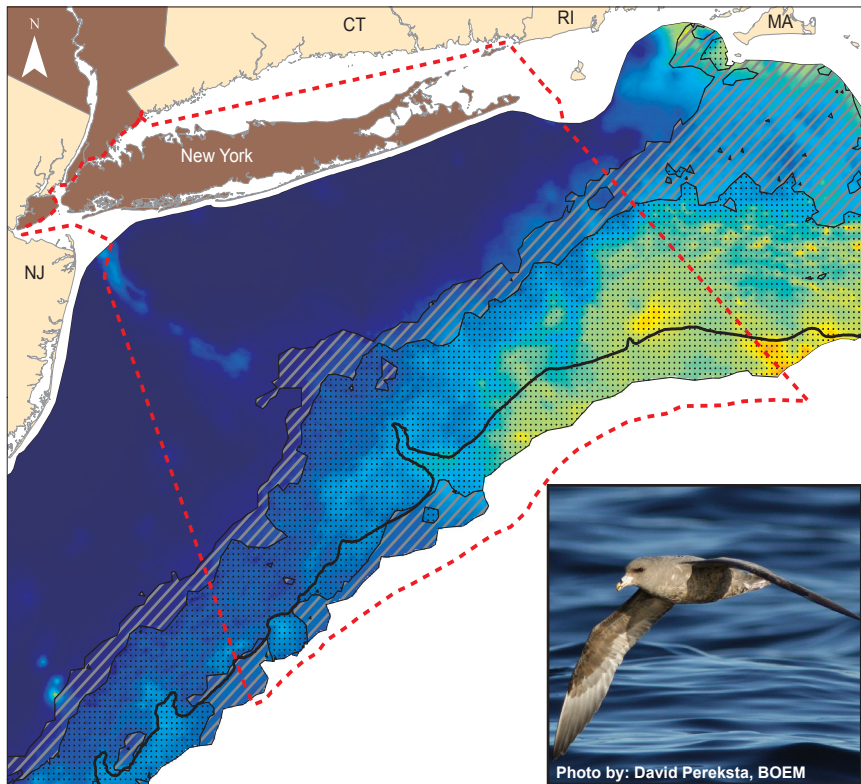


Figure 6.17. Predicted annual average relative index of abundance (SPUE, # indiv./ km²/15-min) for Northern Fulmar, with certainty classes overlaid (see legend in Figure 6.8).

Table 6.36. Data table: Northern Fulmar.

Statistic	SP	SU	FA	WI	All
N obs.	228	43	45	76	392
Freq. (%)	8.9%	1.6%	1.6%	6.6%	4.3%
SPUE when present (No. indiv./ km ² /15 min.)					
Mean	0.63	1.10	0.33	0.58	0.63
10th%ile	0.13	0.23	0.13	0.13	0.13
Median	0.36	0.72	0.26	0.27	0.36
90th%ile	1.21	2.56	0.60	1.02	1.18
Max	13.40	7.20	0.80	5.60	13.40

Table 6.37. Predictor table: Northern Fulmar.

Predictor	Occurrence				Abundance			
	Sp	Su	Fa	Wi	Sp	Su	Fa	Wi
BATH	Green	Green	Red	White	Green	Green	Red	White
SLOPE	Green	Green	White	White	Green	Green	White	White
DIST	Green	Green	White	White	Green	Green	White	White
SSDIST	Green	Green	White	White	Green	Green	White	White
SST	Green	Green	White	White	Green	Green	White	White
STRT	Green	Green	White	White	Green	Green	White	White
TUR	Green	Green	White	White	Green	Green	White	White
CHL	Green	Green	White	White	Green	Green	White	White
ZOO	Green	Green	White	White	Green	Green	White	White
SLPSLP	Green	Green	Red	White	Green	Green	White	White
PHIM	Red	Red	Red	White	Red	Red	White	White

Table 6.38. Diagnostic table: Northern Fulmar.

Diagnostic statistic	Certainty class			
	Low %area 44%	Med. %area 12%	High %area 43%	ALL Avg. MED.
Rank R	Red	Green	n/a	0.21
%1SD	Red	Green	n/a	53.3%
AUC	Green	Green	n/a	0.80
p(AUC)	Green	Green	n/a	0.00
MAPE	Red	Red	n/a	396%
Rel.MAE	Red	Red	n/a	60%
Rel.RMSE	Red	Red	n/a	101%
Rel.Bias	Red	Red	n/a	46%
Bias Dir.	+	+	n/a	+

Northern Gannet (*Morus bassanus*)

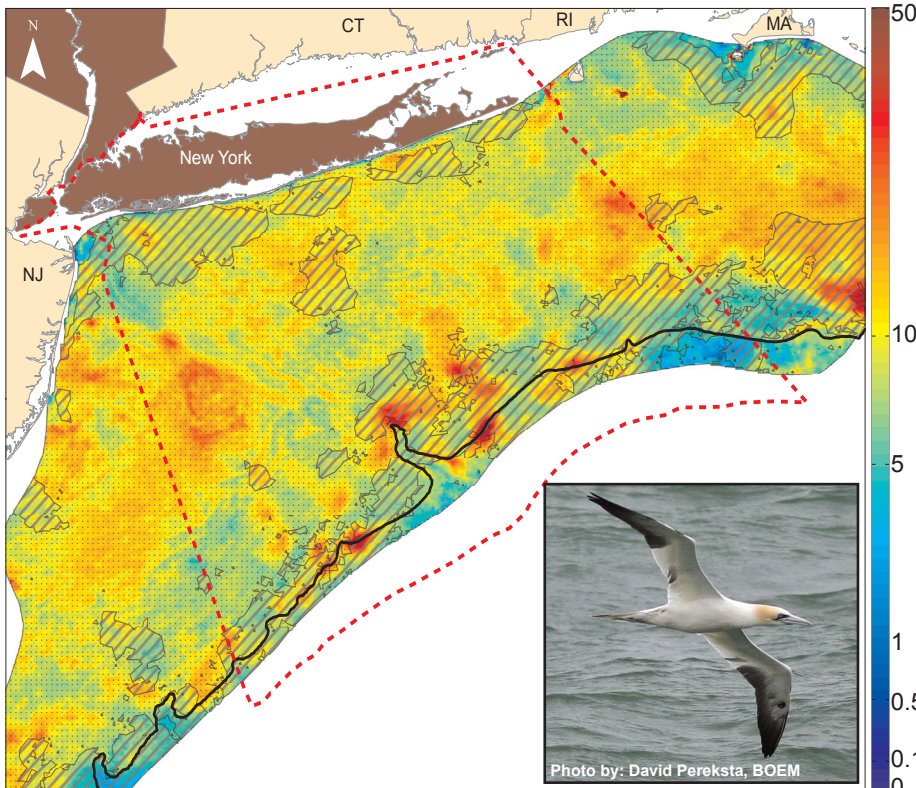


Figure 6.18. Predicted annual average relative index of abundance (SPUE, # indiv./km²/15-min) for Northern Gannet, with certainty classes overlaid (see legend in Figure 6.8).

Table 6.39. Data table: Northern Gannet.

Statistic	SP	SU	FA	WI
N obs.	915	9	385	493
Freq. (%)	35.9%	0.3%	13.9%	42.9%
SPUE when present (No. indiv./km ² /15 min.)				
Mean	18.79	2.98	8.85	10.63
10th%ile	1.80	0.82	1.72	2.73
Median	8.10	2.56	5.40	7.54
90th%ile	40.80	6.48	18.65	20.93
Max	604.30	7.20	104.39	78.39

Table 6.40. Predictor table: Northern Gannet.

Predictor	Occurrence				Abundance			
	Sp	Su	Fa	Wi	Sp	Su	Fa	Wi
BATH								
SLOPE								
DIST								
SSDIST								
SST								
STRT								
TUR								
CHL								
ZOO								
SLPSLP								
PHIM								

Table 6.41. Diagnostic table: Northern Gannet.

Diagnostic statistic	Certainty class			
	Low	Med.	High	ALL
	%area	%area	%area	Avg.
Rank R	62%	35%	3%	LOW
%1SD	0.07	0.30	n/a	0.17
AUC	89.6%	83.3%	n/a	87.9%
p(AUC)	0.59	0.55	n/a	0.64
MAPE	0.20	0.31	n/a	0.01
Rel.MAE	112%	548%	n/a	259%
Rel.RMSE	28%	39%	n/a	32%
Bias Dir.	39%	61%	n/a	48%
	2%	4%	n/a	0%
	-	+	-	

Pomarine Jaeger (*Stercorarius pomarinus*)

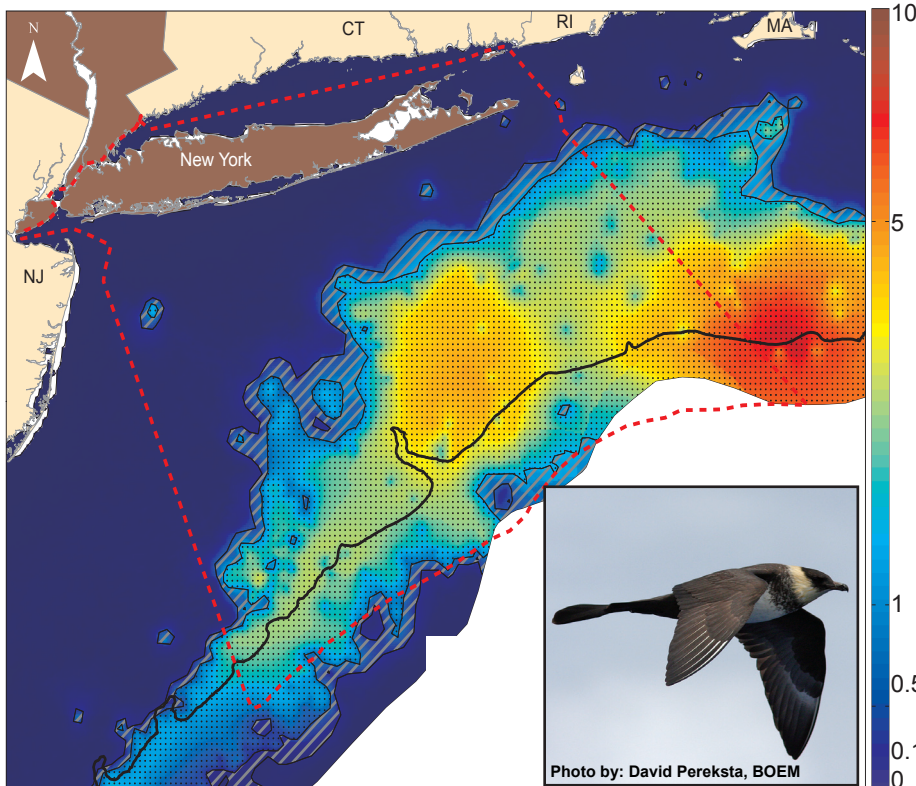


Figure 6.19. Predicted annual average relative index of abundance (SPUE, # indiv./km²/15-min) for Pomarine Jaeger, with certainty classes overlaid (see legend in Figure 6.8).

Table 6.42. Data table: Pomarine Jaeger.

Statistic	SP	SU	FA	WI	All
N obs.	14	6	101	1	122
Freq. (%)	0.5%	0.2%	3.6%	0.1%	1.3%
SPUE when present (No. indiv./km ² /15 min.)					
Mean	1.36	3.67	6.23	0.27	5.50
10th%ile	0.20	0.72	0.20	0.27	0.21
Median	0.36	1.21	3.36	0.27	2.80
90th%ile	4.58	11.89	14.92	0.27	13.35
Max	4.58	12.60	43.20	0.27	43.20

Table 6.43. Predictor table: Pomarine Jaeger.

Predictor	Occurrence				Abundance			
	Sp	Su	Fa	Wi	Sp	Su	Fa	Wi
BATH								
SLOPE								
DIST								
SSDIST								
SST								
STRT								
TUR								
CHL								
ZOO								
SLPSLP								
PHIM								

Table 6.44. Diagnostic table: Pomarine Jaeger.

Diagnostic statistic	Certainty class			
	Low	Med.	High	ALL
	%area	%area	%area	Avg.
Rank R	49%	13%	39%	MED.
%1SD	0.12	0.09	-0.05	0.30
AUC	50.0%	100.0%	80.0%	66.7%
p(AUC)	0.51	0.77	0.73	0.64
MAPE	0.41	0.01	0.00	0.00
Rel.MAE	406%	107%	85%	590%
Rel.RMSE	11%	3%	1%	11%
Bias Dir.	18%	5%	3%	15%
	20%	5%	1%	9%
	+	+	+	+